Novel SARS-CoV-2 specific antibody and neutralization assays reveal wide range of humoral immune response during COVID-19

Mikail Dogan[1], Lina Kozhaya[1], Lindsey Placek[1], Courtney L. Gunter[1], Mesut Yigit[1], Rachel Hardy[1], Matt Plassmeyer[3], Paige Coatney[3], Kimberleigh Lillard[3], Zaheer Bukhari[4], Michael Kleinberg[5], Chelsea Hayes[6], Moshe Arditi[7], Ellen Klapper[6], Noah Merin[8], Bruce T Liang[5], Raavi Gupta[4], Oral Alpan[3] and Derya Unutmaz[1,2]*

[1] Jackson Laboratory for Genomic Medicine, Farmington, Connecticut

[2] Department of Immunology, University of Connecticut School of Medicine, Farmington, CT

[3] Amerimmune, Fairfield, VA

[4] SUNY Downstate Medical Center, Department of Pathology, Brooklyn, NY

[5] Calhoun Cardiology Center, University of Connecticut School of Medicine, Farmington, CT.

[6] Department of Pathology & Laboratory Medicine and Transfusion Medicine
Cedars-Sinai Medical Center, Los Angeles, CA.

[7]Department of Pediatric, Division of Pediatric Infectious Diseases and Immunology, Biomedical Sciences, Cedars-Sinai Medical Center,
Los Angeles, CA 90048.

[8]Department of Internal Medicine, Division of Hematology Cedars-Sinai Medical Center, Los Angeles, CA.

* Corresponding author E-mail: derya@mac.com

Abstract

Development of antibody protection during SARS-CoV-2 infection is a pressing question for public health and for vaccine development. We developed highly sensitive SARS-CoV-2-specific antibody and neutralization assays. SARS-CoV-2 Spike protein or Nucleocapsid protein specific IgG antibodies at titers more than 1:100,000 were detectable in all PCR+ subjects (n=115) and were absent in the negative controls. Other isotype antibodies (IgA, IgG1-4) were also detected. SARS-CoV-2 neutralization was determined in COVID-19 and convalescent plasma at up to 10,000-fold dilution, using Spike protein pseudotyped lentiviruses, which were also blocked by neutralizing antibodies (NAbs). Hospitalized patients had up to 3000-fold higher antibody and neutralization titers compared to outpatients or convalescent plasma donors. Interestingly, some COVID-19 patients also possessed NAbs against SARS-CoV Spike protein pseudovirus. Together these results demonstrate the high specificity and sensitivity of our assays, which may impact understanding the quality or duration of the antibody response during COVID-19 and in determining the effectiveness of potential vaccines.

Introduction

Severe Acute Respiratory Syndrome Coronavirus 2 (SARS-CoV-2), which has caused the COVID-19 pandemic, enters target cells through the interaction of its envelope Spike protein with the primary host cell receptor Angiotensin Converting Enzyme-2 (ACE2), which is then cleaved by a serine protease (TMPRSS2) to allow viral fusion and entry across the cell membrane[1]. Antibodies that can bind to the Spike protein have the potential to neutralize viral entry into cells and are thought to play an important role in the protective immune response to SARS-CoV-2 infection[2-11]

To predict protection against SARS-CoV-2, it is critical to understand the quantity, quality and duration of the antibody responses during different stages of COVID-19 and in the convalescent period. In this regard, assessing the level of neutralizing antibodies (NAbs) that block viral entry into cells could be a critical parameter in determining protection from SARS-CoV-2 and management of convalescent plasma therapies, which are being tested as a COVID-19 treatment option[12-15]. Defining the relationship between disease severity, other individual-specific co-morbidities and the neutralizing antibody responses will be critical in our understanding of COVID-19 and in tailoring effective therapies.

Currently available SARS-CoV-2 antibody tests mostly lack sufficient dynamic range and sensitivity to allow for accurate detection or determination of the magnitude of the antibody response[16]. Furthermore, potential cross-reactivity among SARS-CoV-2 specific antibodies to other endemic coronaviruses could also be confounders in these tests [17-20], thus making them less reliable. Determining neutralization activity in patient plasma also has challenges, as these assays generally rely on live virus replication, requiring a high-level biohazard security BSL-3 level laboratory. Therefore, there is an unmet need to develop sensitive antibody and virus

neutralization assays that are sufficiently robust for screening and monitoring large numbers of SARS-CoV-2 infected or convalescent subjects.

To overcome these experimental challenges, here we developed: 1) Highly sensitive bead-based fluorescent immunoassay for measuring SARS-CoV-2 specific antibody levels and isotypes, and 2) Robust SARS-CoV-2 Spike protein pseudovirus to measure NAb levels in COVID-19 patient plasma. We found striking differences in total antibody levels and neutralization titers between hospitalized or severe COVID-19 patients relative to outpatient or convalescent plasma donors, which were obtained with the purpose of transfer to and treatment of patients. Significant correlations between antibody levels and neutralization titers, age and NAbs to SARS-CoV were also observed. These assays and findings have important implications for assessing the breadth and depth of the humoral immune response during SARS-CoV-2 infection and for the development of effective antibody-based therapies or vaccines.

Results

Development of SARS-CoV-2 specific antibody assay

Determining antibody responses in SARS-CoV-2 infected subjects remains challenging, due to lack of sufficient dynamic range to determine precise antibody titers with antibody isotypes simultaneously. To overcome these obstacles, we developed a fluorescent bead-based immunoassay that takes advantage of the high dynamic range of fluorescent molecules using flow cytometry (Fig. 1a). In this assay, we immobilized biotinylated SARS-CoV-2 Spike protein receptor binding domain (RBD) or the Nucleoprotein (N) on streptavidin beads to detect specific antibodies from patient plasma (Fig. 1a). Different antibody isotypes were measured using anti-Ig (IgG, IgA, IgM, IgG1-4) specific secondary antibodies conjugated to a fluorescent tag (Fig. 1a). Using either anti-S-RBD antibody or soluble ACE2-Fc, we show very high sensitivity in detecting

Spike protein binding, down to picogram ranges (Fig. 1b). Similarly, S-RBD-specific antibodies were detectable in serial dilutions up to 100,000-fold of plasma samples from SARS-CoV-2 PCR+ subjects at high specificity and sensitivity (Fig. 1c). We then used the titration curves from COVID-19 convalescent and healthy control plasma to normalize the area under the curve (AUC) values to quantitate the antibody levels (Supplementary Fig. 1a). Negative threshold values were set using healthy control AUC levels plus one standard deviation of the mean.

In addition to S-RBD and Nucleocapsid protein, we also attached different viral components such as S1 subunit of Spike protein, S1 subunit N Terminal Domain (NTD) and S2 Extracellular Domain (ECD) onto the magnetic beads and tested IgG levels specific to those viral proteins to compare the antibody levels they detect. Interestingly, S-RBD captured significantly more antibodies compared to S1 which is the subunit of Spike protein that contains S-RBD (Fig. 1d).

We also evaluated the dynamic range of our assay by screening some of the plasma samples with a commercial ELISA-based antibody assay next to our bead-based assay and comparing the detected antibody levels. Antibody levels from the two antibody assays showed a high correlation (r_s = 0.86), confirming our assay's precision, and the bead-based antibody assay showed a wider dynamic range compared to the ELISA-based assay. (Fig. 1e)

Using bead-based assay, we screened COVID-19 patient or convalescent plasma samples (Table-1; n=115) for total S-RBD and Nucleocapsid specific IgG AUC values of COVID-19 positive subjects, which varied 3-logs from ~10^4 to ~10^7 (Fig. 2a). S-RBD specific IgM (40/40) and IgA (115/115) were also detectable and above the negative control threshold in all subjects (Fig. 2a). Statistical sensitivity and specificity estimates of our bead-based antibody assays were 100% and 99.34% for S-RBD IgG; 100% and 90.9% for S-RBD IgM, 94.26% and 87.87% for S-RBD IgA and

99.13% and 94.93% for Nucleocapsid IgG, respectively. Furthermore; S1 subunit, S1 N Terminal Domain (NTD), S2 Extracellular Domain (ECD) and Nucleocapsid protein-specific IgG and S-RBD specific IgA levels positively correlated with S-RBD IgG antibodies (Supplementary Fig. 1b, c) with the highest correlation with S1 IgG (r_s = 0.987). Notably, IgG1 subclass antibody levels were comparable to total IgG levels whereas the other subtypes were relatively lower (Fig. 2b). There were significant differences in S-RBD or Nucleocapsid antibody levels between outpatient, hospitalized, and ICU/deceased subjects, with the highest levels observed in the most severe cases (Fig. 2c, d, e). Importantly, subjects who had recovered from COVID-19 and were also potential donors for convalescent plasma therapy (hereafter referred to as plasma donors), also had significantly lower antibody titers than hospitalized, intensive care unit (ICU) or deceased patients (Fig. 2c, d, e). Overall, individual S-RBD and Nucleocapsid IgG levels appeared to correlate with their IgA and IgG subclass (IgG1-4) responses to S-RBD (Supplementary Fig. 1d). Subdividing the subjects by sex did not reveal any statistical difference in IgG levels at any of the disease stages (Fig. 2f).

Table 1. Characteristics of SARS-CoV-2 infected and control subjects

Demographics		Healthy Controls (n=56)	Negative (n=94)	Outpatient (n=39)	Hospitalized (n=19)	ICU/Deceased (n=24)	Plasma Donors (n=33)
Sex	Male	14	33	11	7	10	18
	Female	42	61	28	12	14	15
Age	Mean (+-SEM)	45.5 (+-1.78)	54.1 (+-1.97)	46.0 (+-2.20)	62.2 (+-3.41)	68.0 (+-1.87)	45.5 (+-1.99)
	Median	47.0	59.0	47.0	63.0	70.0	48.0
Days between PCR/Blood	Mean (+-SEM)	N/A	N/A	40.7 (+-2.79)	21.0 (+-3.28)	25.8 (+-3.17)	65.4 (+-1.68)
	Median	N/A	N/A	43.0	28.0	24.5	66.0

Development of SARS-CoV-2 Spike protein pseudovirus

Next, we sought to develop a sensitive and high throughput SARS-CoV-2 neutralization assay by incorporating SARS-CoV-2 Spike protein into lentiviruses to assess specific inhibition of viral entry. To produce Spike protein pseudotyped lentiviral particles, we first ensured expression of the Spike protein on the cell membrane of transfected 293 cells, from which it would incorporate into the lentiviruses. Human codon optimized SARS-CoV-2 Spike protein sequences with and without endoplasmic reticulum retention signal (ERRS), which would be predicted to be more efficiently expressed on the cell surface membranes, were cloned into an expression vector and transfected into 293 cells. To evaluate membrane expression of Spike protein, cells were stained with recombinant soluble ACE2-Fc fusion protein followed by a secondary staining with an anti-Fc antibody (Fig 3a). The percentage of Spike protein over-expressing cells was similar in the presence or absence of ERRS, but cells expressing Spike protein without ERRS showed a higher geometric mean of expression (Fig. 3b). As such, we used Spike protein lacking the ERRS for lentiviral pseudotyping to ensure its higher incorporation onto viral membranes.

We then co-transfected 293 cells with replication defective lentivectors encoding GFP or RFP reporter genes and the Spike protein encoding plasmid and harvested the supernatant at 24 hours, which was then used to infect cells expressing ACE2 (Fig. 3c). Bald particles were generated by transfecting lentivirus plasmids without any envelope and used as a negative control. Next, we tested the transduction efficiency of the viruses on wild type 293 cells, given they express low levels of endogenous ACE2 (Supplementary Fig. 2a, b). While we found clearly defined infection of 293 cells with Spike-protein pseudovirus compared to bald virions, infection rate determined by GFP or RFP expression was relatively low (Fig. 3d). We therefore generated human-ACE2 over-expressing 293 cells with a GFP reporter (ACE2-IRES-GFP) or fused to fluorescent mKO2 protein (ACE2-mKO2). ACE2 overexpression of ACE2-IRES-GFP or ACE2-

mKO2 was confirmed by staining with SARS-CoV-2 Spike-protein S1 subunit fused with mouse Fc (mFc) and anti-mFc secondary antibody (Supplementary Fig. 2a, b). Indeed, these ACE2 over-expressing 293 cells (293-ACE2) were efficiently transduced with Spike protein pseudoviruses encoding either GFP or RFP (Fig. 3e). The efficiency of Spike-protein pseudovirus infection was comparable in ACE2-IRES-GFP or ACE2-mKO2 fusion protein (Fig. 3e), and therefore both were used in subsequent neutralization experiments. In addition, we developed SARS-CoV Spike protein pseudotyped lentivirus, which similarly infected 293-ACE2 cells at almost 100% efficiency at higher virus supernatant volumes (Fig. 3f). We also tested the stabilities of SARS-CoV-2 and SARS-CoV Spike protein pseudotyped lentiviruses after serial freeze/thaw cycles and found that their infectivity remained mostly similar with little loss of activity after 3 cycles (Fig. 3f).

Neutralization of SARS-CoV-2 Spike protein pseudovirus with soluble ACE2, NAbs and COVID-19 plasma

We next investigated whether Spike protein pseudoviruses could be neutralized by soluble ACE2 (sACE) or Spike protein specific NAbs (Fig. 4a). For this experiment, Spike protein pseudotyped SARS-CoV-2 and SARS-CoV pseudoviruses were pre-cultured with different concentrations of sACE2 or NAbs, then added to 293-ACE2 cells. Subsequently, infection was determined 3 days post-infection based on GFP or RFP expression as described above. sACE2 neutralized both SARS-CoV-2 and SARS-CoV pseudovirus infections in a dose dependent manner (Fig. 4b, c), although neutralization of SARS-CoV-2 was slightly better than that of SARS-CoV pseudoviruses (Fig. 4b, c, and Supplementary Fig. 3a). Furthermore, Spike-RBD specific NAb neutralized SARS-CoV-2 pseudovirus entry much more efficiently than sACE2 but had no effect on SARS-CoV pseudovirus (Fig. 4c). One of the SARS-CoV-2 S-RBD specific antibodies (non-NAb) did not show any neutralization of SARS-CoV-2, however very low level neutralization of SARS-CoV pseudovirus was detected (Fig. 4c). We also observed measurable differences in the neutralizing

activity of four different NAbs and two different soluble ACE2 proteins from different sources (Fig. 4d), showing the utility of this assay for such screening. Taken together, these experiments demonstrate that the combination of pseudotyped viruses and 293-ACE2 cells can be used to generate highly sensitive SARS-CoV-2 and SARS-CoV neutralization assays.

Using this approach, we then tested neutralization titers from COVID-19 patients or seropositive donors with serial dilution of their plasma. Accordingly, plasma samples in 3-fold serial dilutions were incubated with Spike pseudovirus and added to 293-ACE2 cells and infection was determined as described in Figure 4. Healthy control plasma samples were used as negative controls whereas anti-S-RBD NAb served as a positive control (Fig. 5a). None of the control plasma (n=34, 1 shown in Fig. 5a) tested showed any neutralization activity, whereas patient plasma efficiently neutralized the virus at up to 10,000-fold serial dilution (Fig. 5a). The 50% neutralization titer (NT50), was determined using the half-maximal inhibitory concentration values of plasma samples, normalized to control infections, from their serial dilutions. Importantly, the NT50 values of the subjects were much higher in hospitalized patients than in outpatients (Fig. 5b). NT50 values for hospitalized and ICU/deceased subjects were also up to 1000-fold higher than convalescent plasma donors (Fig. 5b). Hospitalized males and females, separately, also remained higher in their NT50 levels and no difference was observed within each group (Fig. 5c).

We also tested whether SARS-CoV-2 PCR+ plasma could neutralize the SARS-CoV pseudovirus. 104 plasma samples from all groups were tested for their ability to neutralize SARS-CoV-2 and SARS-CoV pseudoviruses. Remarkably, most of the plasma samples also neutralized SARS-CoV pseudovirus, although less efficiently than SARS-CoV-2 pseudovirus (Fig. 5d). Interestingly, NT50 levels of plasma samples for SARS-CoV-2 and SARS-CoV significantly correlated in hospitalized subjects (Fig. 5e), whereas there were no correlations in outpatients and plasma

donors or when all groups were combined (Supplementary Fig. 5a). Additionally, when we compared the severity groups for their SARS-CoV NT50 values, we did not observe any significant difference between the groups (Supplementary Fig. 5b).

Correlations of SARS-CoV-2 neutralization, antibody levels and COVID-19 subject characteristics

To better understand the associations between patient characteristics and the humoral immune response in COVID-19, we next determined correlations between antibody AUC levels, NT50 values and demographics of the study subjects. First, we assessed the correlation between NT50 values with S-RBD or Nucleocapsid antibody titers or their subclasses. All Igs including S-RBD IgG (r_s = 0.81), Nucleocapsid IgG (r_s = 0.689), S-RBD IgA (r_s = 0.60) and S-RBD IgM (r_s = 0.47) showed significant correlation with NT50 values of each subject (Fig. 6a). Among Ig subclasses specific to S-RBD; IgG1 (r_s = 0.80), IgG3 (r_s = 0.69) and IgG2 (r_s = 0.67) and, to a lesser degree, IgG4 (r_s = 0.51) also correlated with NT50 values (Fig. 6b). Total S-RBD IgG also correlated in a similar fashion with other IgG isotypes, with IgG1 showing the highest positive correlation (r_s = 0.96) (Supplementary Fig. 4a).

Next, we correlated the antibody AUC levels and NT50 values of the subjects with their age. Subjects had significantly higher S-RBD IgG (r_s = 0.53), Nucleocapsid IgG (r_s = 0.43), S-RBD IgA (r_s = 0.41) and NT50 (r_s = 0.579) values, as their age increased (Fig. 6c).

We also explored the relationship of the number of days between PCR test result and blood draw with antibody levels or NT50 values, excluding the subjects that had 15 days or fewer between those dates to ensure that antibody levels had already reached their peak. Of note, there was no

correlation between the number of days and the IgG to S-RBD or the NT50 (Supplementary Fig. 4b), suggesting a potential persistence in antibody titers at least for 3 month duration in this cohort.

Discussion

The COVID-19 pandemic is continuing to spread globally unabated, including within the United States. There is an urgent need to better understand the immune response to the virus so that effective immune-based treatments and vaccines can be developed[21,22]. Neutralization of the virus by antibodies (NAbs) is one of the goals to achieve protection against SARS-CoV-2[23]. Despite rapid development of many serological tests, important questions about the quality and quantity of seroprevalence in individuals remains still unclear[24,25]. Here, we developed highly sensitive and specific humoral assays that measure both the magnitude and neutralization capacity of antibody responses in COVID-19 patients. Every SARS-CoV-2 infected subject we tested (n=115) had detectable antibodies and all subjects except one exhibited neutralization; both of these qualities were completely absent in non-infected controls. However, there was a profound difference in antibody and neutralization titers among subjects, ranging in more than 1000-fold differences. Furthermore, we found that almost all COVID-19 patients also had neutralizing antibodies for SARS-CoV, suggesting a high degree of cross-reactivity between these two virus Spike proteins.

One of our key findings was clustering of antibody responses based on severity of the disease; as hospitalized patients showed much higher antibody levels and neutralization capacity than outpatient subjects or convalescent plasma donors. This finding is consistent with recent reports suggesting that patients with more severe disease contain relatively higher levels of antibodies for SARS-CoV-2 infection[2,26-30]. Interestingly, most of the convalescent plasma donors had much lower levels of neutralizing antibodies (by at least an order of magnitude) than hospitalized

patients, who would be the suitable recipients for such plasma transfer therapy. This finding raises the question of whether convalescent plasma transfers may actually provide benefit to severe COVID-19 patients by providing neutralizing antibodies. It may perhaps be more beneficial to identify donors with much higher neutralizing antibody titers for the plasma donation. As such, our findings point to the importance of having access to assays that have a large dynamic range to detect antibody responses in COVID-19 patients or seropositive individuals. This neutralization assay also revealed differences in commercial antibodies to SARS-CoV-2 in their capacity to block virus entry, and as such can be used for rapid identification or generation of synthetic NAbs. In addition to measuring neutralization titers, the pseudoviruses can be used to probe cells that have the potential to be infected with SARS-CoV-2, given lentiviruses can infect most cell types and do not require cell division to integrate into the genome. This infection assay may also be used to screen small molecules that may impact virus cell entry.

Along with SARS-CoV-2, we also developed a pseudotyped lentivirus with SARS-CoV Spike protein, which was equally efficient at infecting ACE2 overexpressing cells. This finding is consistent with results that SARS-CoV-2 Spike protein in complex binding with human ACE2 (hACE2) is similar overall to that observed for SARS-CoV[31]. There was however slightly better neutralization of SARS-CoV-2 cell entry than SARS-CoV with soluble ACE2, which could be due to key residue substitutions in SARS-CoV-2, creating a slightly stronger interaction and thus higher affinity for receptor binding than SARS-CoV Spike protein[31]. Accordingly, we also tested the ability of COVID-19 patient plasma for SARS-CoV neutralizing capacity and found significant SARS-CoV specific neutralization in COVID-19 patients. However, the neutralization titers for SARS-CoV were significantly lower and there was no correlation with the neutralization activity against SARS-CoV-2 when all severity groups were combined. Indeed, some donors even had relatively higher SARS-CoV neutralization (Fig. 5e). Although there was significant correlation

between SARS-CoV-2 and SARS-CoV NT50 levels when hospitalized and ICU/Deceased subjects were analyzed separately. Given that the two viruses share ~75% identical amino acid sequences in their Spike proteins and there are conserved epitopes between them[32], it is conceivable that some of the SARS-CoV-2 NAbs have cross-neutralizing activity[33,34]. It is noteworthy that a recent study showed a NAb developed for SARS-CoV was highly effective at neutralizing SARS-CoV-2[35]. It is also tempting to speculate that presence of SARS-CoV specific NAbs could be more potent perhaps by targeting highly conserved regions of the Spike protein, making it more difficult for the virus to select for escape mutants.

Other antibody and neutralization assays have been developed during the submission of our manuscript[2,3,9,36-40]. Although direct comparison is difficult due to differences in the assay methodologies and different sample sets, we believe our assays embody distinctive features that further enhance this critically important immune response to SARS-CoV-2. The use of the flow cytometry bead based fluorescent system that detects Spike or Nucleocapsid protein bound antibodies provides a high-throughput assay with a very high dynamic range and sensitivity, as it could detect antibodies from some subjects at up to a million-fold dilution of the plasma. This assay is also scalable and can be easily adaptable to other viral antigens. Using a flow cytometry platform is also important in that the assay can be further developed in a single panel to identify all antibody isotypes simultaneously and to complement flow cytometric immune phenotyping of COVID-19 patients. The high sensitivity and specificity of our assay has allowed us to correlate the Spike protein RBD-specific antibody levels with neutralization titers, which showed very high concordance, and thus can be utilized as a proxy for neutralization in a clinical setting. Furthermore, the bead-based immunoassay can also be further developed to screen for antibodies reacting to other SARS-CoV-2 antigens simultaneously and can be useful in identifying antibodies that cross-react between different species of coronavirus proteins. Determining other

isotypes such as IgA and IgG subclasses may also help in future mechanistic studies. It is clear that the dominant antibody response in almost all donors was IgG1, but some also show high IgA and IgG2-4, at varying levels. For example, given the importance of IgA antibodies in providing immunity on mucosal surfaces within the respiratory system, SARS-CoV-2 RBD-spike protein specific IgA levels may also play an important role in the upper and lower respiratory system, or perhaps also in the gut, of COVID-19 patients[41,42].

There are also several potential practical implications to our findings. First, the patient population with the greatest risk factors for severe outcomes from infection such as age and co-morbid conditions had the highest antibody titers as well as neutralization of the virus. This is also the case for those patients who had lethal disease. It is therefore possible that surviving COVID-19 may require non-antibody dependent factors or that producing too much antibody may even have deleterious effects[43], such as potential antibody-dependent enhancement phenomenon by triggering Fc receptors on macrophages[44]. In this regard, it is interesting to note that a Bruton tyrosine kinase (BTK) inhibitor that targets Fc-receptor signaling in macrophages is being tested in a randomized clinical trial [45]. Thus, understanding the mechanism of survival from COVID-19 and immune response dynamics will be critical in the better prediction of outcomes as well as in assaying for a protective response to potential vaccines.

In conclusion, the assays developed herein can have utility in uncovering dynamic changes in the antibody levels in SARS-CoV-2 infected subjects over time, in responses to vaccines and as potential clinical determinants for plasma or antibody therapies for COVID-19 patients.

Materials and Methods

Participants

COVID-19 subjects (n=115) were recruited at SUNY Downstate Medical Center, New York, NY, Cedars Sinai, Los Angeles, CA, or the University of Connecticut, School of Medicine, Farmington CT following testing and/or admission for COVID-19 infection. Written informed consent was obtained from all participants in this study and was approved by the following IRBs: 1) IRB# SUNY:269846. The patients were recruited at SUNY Downstate, NY and processed and biobanked at Amerimmune, Fairfax VA; 2) IRB# STUDY00000640. Convalescent plasma was collected at Cedars Sinai Medical Center according to FDA protocol (https://www.fda.gov/vaccines-blood-biologics/investigational-new-drug-ind-or-device-exemption-ide-process-cber/recommendations-investigational-covid-19-convalescent-plasma#Collection%20of%20COVID-19). The source of the convalescent plasma was volunteer blood donors who were recovered from COVID-19. Donors met routine blood donor eligibility requirements established by the FDA and had a prior SARS-CoV-2 infection documented by a laboratory test for the virus during illness, or antibodies to the virus after recovery of suspected disease. All donors were at least 28 days from either resolution of COVID-19 symptoms or diagnostic clearance, whichever was longer; 3) IRB# 20-186-1. UConn Healthcare workers who tested positive for the virus by PCR were recruited and samples banked for future testing. 4) IRB#: 17-JGM-13-JGM or 16-JGM-06-JGM. De-identified control subjects (n=56) with previously frozen (more than a year ago) samples obtained from healthy controls or determined to be SARS-CoV-2 PCR negative (IRB SUNY:269846). All antibody assays were performed at the Jackson Laboratory for Genomic Medicine, Farmington, CT. Subject characteristics are shown in Table 1. All plasma samples were aliquoted and stored at -80°C. Prior to experiments, aliquots of plasma samples were heat-inactivated at 56°C for 30 minutes.

Over-expression of SARS-CoV-2 Spike protein and cell culture

Human codon optimized SARS-CoV-2 Spike protein sequence was synthesized by MolecularCloud (MC_0101081). 5'-ACGACGGAATTCATGTTCGTCTTCCTGGTCCTG-3' and 5'-ACGACGGAATTCTTAACAGCAGGAGCCACAGC-3' primers were used to amplify the SARS-CoV-2 Spike protein sequence without Endoplasmic Reticulum Retention Signal that is the last 19 amino acids[33]. Full length and truncated SARS-CoV-2 spike protein sequences were then cloned into pLP/VSVG plasmid from Thermo Fisher under CMV promoter after removing the VSVG sequence via EcoRI-EcoRI restriction digestion. HEK-293T cells (ATCC; mycoplasma-free low passage stock) were transfected with the expression plasmids using Lipofectamine 3000 (Invitrogen) according to the manufacturer's protocol as previously described[46]. The cells were cultured in complete RPMI 1640 medium (RPMI 1640 supplemented with 10% FBS; Atlanta Biologicals, Lawrenceville, GA), 8% GlutaMAX (Life Technologies), 8% sodium pyruvate, 8% MEM vitamins, 8% MEM nonessential amino acid, and 1% penicillin/streptomycin (all from Corning Cellgro) for 72 hours, collected using %0.05 Trypsin-0.53 mM EDTA (Corning Cellgro) and stained with Biotinylated Human ACE2 / ACEH Protein, Fc,Avitag (Acro Biosystems) then stained with APC anti-human IgG Fc Antibody clone HP6017 (Biolegend). Samples were acquired on a BD FACSymphony A5 analyzer and data were analyzed using FlowJo (Tree Star).

Pseudotyped lentivirus production and titer measurement

Lentivector plasmids containing RFP or GFP reporter gene**s** were co-transfected with either SARS-CoV-2 Spike protein or SARS**-CoV** Spike protein (Human SARS coronavirus (SARS-CoV) Spike glycoprotein Gene ORF cDNA clone expression plasmid (Codon Optimized) from SinoBiological) plasmids into HEK-293T cells using Lipofectamine TM 3000 (Invitrogen) according to the manufacturer's protocol**.** Viral supernatants were collected 24-48 hours post-

386 transfection, filtered through a 0.45 µm syringe filter (Millipore) to remove cellular debris, and
387 concentrated with Lenti-X (Invitrogen) according to the manufacturers protocol. Lentivirus
388 supernatant stocks were aliquoted and stored at −80°C. To measure viral titers, virus preps were
389 serially diluted on ACE2 over-expressing 293 cells. 72 hours after infection, GFP or RFP positive
390 cells were counted using flow cytometry and the number of cells transduced with virus
391 supernatant was calculated as infectious units/per m**L**.
392

393 ## Generating human ACE2 over-expressing cells

394 Wildtype ACE2 sequence was obtained from Ensembl Gene Browser (Transcript ID:
395 ENST00000252519.8) and codon optimized with SnapGene by removing restriction enzyme
396 recognition sites that are necessary for subsequent molecular cloning steps, preserving the amino
397 acid sequence. The sequence of mKO2 (monomeric Kusabira-Orange-2[47]) obtained from
398 Addgene (#54625)[48], and was added onto the C terminal end of ACE2 before the stop codon with
399 a small linker peptide (ccggtcgccacc) encoding the amino acids “PVAT”. The fusion constructs
400 were synthesized via GenScript and cloned into a lentiviral vector lacking a fluorescent reporter.
401 The full length human ACE2 sequence without fusion fluorescent proteins was amplified from the
402 ACE2-mKO2 fusion construct using 5’-ACGACGGCGGCCGCATGTCAAGCTCTTCCTGGC-3’
403 and 5’- ACGACGGAATTCTTAAAAGGAGGTCTGAACATCATCAG-3’ primers, generating a stop
404 codon at the C-terminus, and then cloned into a lentiviral vector encoding GFP reporter separated
405 from multiple cloning site via an internal ribosome entry site (IRES) sequence. To determine the
406 virus titers, HEK-293T cells were transduced with full length ACE2-IRES-GFP, ACE2-mKO2
407 fusion construct lentiviruses and analyzed via flow cytometry for their reporter gene expression
408 72 hours after infection. WT and ACE2 over-expressing HEK-293T were also stained with SARS-
409 CoV-2 S1 protein, Mouse IgG2a Fc Tag (Acro Biosystems) followed with APC Goat anti-mouse

410 IgG2a Fc Antibody (Invitrogen). Samples were acquired on a BD FACSymphony A5 analyzer and
411 data were analyzed using FlowJo (BD Biosciences).
412

413 ## SARS-CoV-2 antibody detection using Flow immunoassay

414 To screen for antibody binding to SARS-CoV-2 proteins, The DevScreen SAv Bead kit (Essen
415 BioScience, MI) was used. Biotinylated 2019-nCoV (COVID-19) Spike protein RBD, His, Avitag,
416 Biotinylated CoV-2 (COVID-19) Nucleocapsid protein, His,Avitag, Biotinylated CoV-2 (COVID-19)
417 S1 protein, His,Avitag (Acro Biosystems, DE), Biotinylated SARS-CoV-2 (2019-nCoV) Spike S1
418 NTD-His & AVI recombinant protein and Biotinylated SARS-CoV-2 (2019-nCoV) Spike S2 ECD-
419 His recombinant protein (Sino Biological Inc.) were coated to SAv Beads according to
420 manufacturer's instructions. Confirmation of successful bead conjugation was determined by
421 staining with anti-His Tag (Biolegend) and flow cytometry analysis. S-RBD, N, S1, S1-NTD and
422 S2-ECD conjugated beads were then used as capture beads in flow immunoassay where they
423 were incubated with anti-S-RBD human IgG positive control (provided in GenScript SARS-CoV-
424 2 Spike S1-RBD IgG & IgM ELISA Detection Kit as positive control), recombinant Human ACE2-
425 Fc (Acro Biosystems) or plasma and serum samples for 1 hour at room temperature. Plasma
426 samples were assayed at a 1:100 starting dilution and 3 additional 10-fold serial dilutions. Anti-S-
427 RBD antibody and ACE2-Fc were both tested at a 5 μg/mL starting concentration and in additional
428 5-fold serial dilutions. Detection reagent was prepared using Phycoerythrin-conjugated anti-
429 human IgG Fc clone HP6017, anti-human IgM clone MHM-88 (Biolegend), anti-human IgA clone
430 IS11-8E10, anti-human IgG1 clone IS11-12E4.23.20 (Miltenyi Biotec), anti-human IgG2 Fc clone
431 HP6002, anti-human IgG3 Hinge clone HP6050 and anti-human IgG4 pFc clone HP6023
432 (Southern Biotech), added to the wells and incubated for another hour at room temperature.
433 Plates were then washed twice with PBS and analyzed by flow cytometry using iQue Screener
434 Plus (IntelliCyt, MI). Flow cytometry data were analyzed using FlowJo (BD biosciences).

Geometric means of PE fluorescence in different titrations were used to generate the titration curve and 20 healthy control plasma were used to normalize the area under the curve (AUC). Statistical analyses were performed using GraphPad Prism 8.0 software (GraphPad Software).

SARS-CoV-2 antibody detection using ELISA

To evaluate antibodies binding to CoV-2 S-RBD protein, SARS-CoV-2 Spike S1-RBD IgG and IgM ELISA Detection Kit from GenScript was used according to the manufacturer's instructions. Absorbance was measured at 450 nm using an Epoch 2 microplate spectrophotometer (BioTek).

Pseudotyped virus neutralization assay

Three-fold serially diluted monoclonal antibodies including anti-SARS-CoV-2 Neutralizing human IgG1 Antibody from Acro Biosystems, NAb#1 (Fig 4c, d), GenScript clone ID 6D11F2, NAb#2 (Fig 4d) and GenScript clone ID 10G6H5, NAb#3 (Fig 4d), Invitrogen clone ID MA5-35939 Nab#4 (Fig 4d), recombinant human ACE2-Fc (Acro Biosystems, sACE2#1 and GenScript, sACE2#2 (Fig 4d) or plasma from COVID-19 convalescent individuals and healthy donors were incubated with RFP-encoding SARS-CoV-2 or GFP-encoding SARS-CoV pseudotyped virus with 0.2 multiplicity of infection (MOI) for 1 hour at 37°C degrees. The mixture was subsequently incubated with 293-ACE2 cells for 72h hours after which cells were collected, washed with FACS buffer (1xPBS+2% FBS) and analyzed by flow cytometry using BD FACSymphony A5 analyzer. Percent infection obtained was normalized for samples derived from cells infected with SARS-CoV-2 or SARS-CoV pseudotyped virus in the absence of plasma, ACE2-Fc or monoclonal antibodies. The half-maximal inhibitory concentration for plasma (NT50), ACE2-Fc or monoclonal antibodies (IC50) was determined using 4-parameter nonlinear regression (GraphPad Prism 8.0).

Statistical Analyses

All statistical analyses were performed using GraphPad Prism V8 software. Continuous variable datasets were analyzed by Mann-Whitney U test for non-parametric datasets when comparing clinical groups, and exact P values are reported. Spearman p analysis was used to determine the relationship existing between two sets of non-parametric data, where a value of 0 indicated no relationship, values between 0 and +/-0.3 indicated a weak relationship, values between +/-0.3 and +/-0.7 indicated a moderate relationship, values between +/-0.7 and +/-1.0 indicated a strong relationship, and a value of +/-1.0 indicated a perfect relationship between sets of data. [49]

Data availability

The source data for the Figures along with the Supplementary Figures presented in this paper are available upon request.

Acknowledgements

The research in this study was supported by National Institute of Health (NIH) grants R01AI121920, U54 NS105539 and U19 AI142733 to D.U. We thank Tina Vaziri for critical reading.

Author contributions

M.D., L.K. and D.U. conceived and designed the experiments. M.D., L.K., L.P., M.Y. and R.H. carried out the experiments. B.T.L. designed the clinical research study on UConn Healthcare

483 workers and M.K. recruited participants and executed clinical protocols. R.G. and O.A designed
484 the clinical research study at SUNY State Medical Center, Z.B., M.B, P.C and K.L, recruited,
485 processed, coordinated and executed the clinical protocols. M.A., E.K., N.M. and C.H, designed,
486 recruited and stored convalescent plasma samples at Cedars Sinai hospital. M.D., L.K, C.L.G.
487 and D.U. analyzed the data, performed statistics, drew illustrations and prepared the figures. M.D.
488 and D.U. wrote the manuscript.
489
490

491 Figure Legends

492

493 **Figure 1: SARS-CoV-2 specific antibody detection assay.**

494 **a.** Illustration of antibody detection assay. Biotinylated S-RBD or Nucleocapsid proteins are
495 captured by streptavidin coated beads, then incubated with plasma samples and stained with PE
496 conjugated anti-IgG, IgA, IgM, IgG1, IgG2, IgG3, IgG4 antibodies. Fluorescence intensity
497 analyzed by flow cytometry. **b.** Histogram overlays demonstrating the detection of anti-S-RBD
498 human IgG antibody (left) and soluble ACE2-Fc (right) as positive controls for plasma antibody
499 assay. **c**. Representative patient plasma titration. Healthy control plasma at 1:100 dilution was
500 used as a negative control**.** Serial dilutions were used in the flow cytometry overlay. **d.**
501 Comparison of IgG antibody levels captured by S-RBD, S1 Subunit of Spike, S1 N Terminal
502 Domain (NTD), S2 Extracellular Domain (ECD) and Nucleocapsid Protein coated beads. **e**.
503 Correlation and comparison of bead-based assay S-RBD IgG antibody levels with ELISA-based
504 assay. Two-tailed Mann-Whitney U test was used to determine the statistical significance in figure
505 **d** and two-tailed Spearman's was used for correlation significance in figure **e**. Horizontal bars in
506 **d** and **e** indicate mean values.
507

Figure 2: SARS-CoV-2 specific antibody detection in COVID-19 and convalescent plasma samples.

a. Measurement of Spike protein and Nucleocapsid protein specific IgG and Spike protein specific IgM and IgA antibodies as described in Figure 1. Area under the curve (AUC) values of plasma antibodies were calculated from reciprocal dilution curves in antibody detection assay. Dotted lines indicate the negative threshold calculated by adding 1 standard deviation to the mean AUC values of healthy controls' plasma. Horizontal bars indicate the mean. **b.** S-RBD specific IgG subclass AUC levels. **c.** S-RBD IgG AUC values of subject plasma grouped by outpatient, hospitalized, ICU or deceased and plasma donors. **d.** Nucleocapsid protein IgG AUC values of subject plasma grouped by outpatient, hospitalized, ICU or deceased and convalescent plasma donors. **e.** S-RBD IgA AUC values of subject plasma grouped by outpatient, hospitalized, ICU or deceased and plasma donors. **f.** S-RBD IgG AUC values of severity groups and plasma donors subdivided into males and females. Statistical significances were determined using two-tailed Mann-Whitney U test.

Figure 3: Development of SARS-CoV-2 and SARS-CoV Spike protein pseudotyped lentiviruses.

a. Schematic illustration of Spike protein expression on the cell surface and soluble ACE2-Fc staining followed by an anti-Fc antibody staining. **b.** 293 cells transfected with Spike protein with or without endoplasmic reticulum retention signal (ERRS) or with VSV-G as a negative control. The cells were stained with ACE2-Fc and anti-Fc-APC secondary antibody, flow cytometry data overlays are shown. **c.** Schematic representation of Spike protein pseudovirus generation and subsequent infection of ACE2-expressing host cells. A lentivector plasmid and a Spike protein over-expressing envelope plasmid are used to co-transfect 293 cells to generate Spike pseudovirus that in turn infect engineered cells over-expressing wild type ACE2 or ACE2-mKO2

fusion. **d.** Infection of wild type 293 cells with either bald lentiviruses generated without envelope plasmid or Spike protein pseudovirus. **e.** Infection of 293-ACE2 cells with bald and Spike lentiviruses. GFP and mKO2 markers are used to determine ACE2 over-expressing cells in ACE2-IRES-GFP and ACE2-mKO2, respectively. **f.** The titrations of SARS-CoV-2 and SARS-CoV Spike protein pseudoviruses encoding RFP. ACE2-IRES-GFP expressing 293 cells were incubated with 3-fold serial dilutions of virus supernatant, stored for several hours at 4°C or serially frozen and thawed for 1, 2 and 3 cycles, and analyzed for RFP expression by flow cytometry on day 3 post-infection. Percent infection is % RFP+ cells after gating on GFP+ cells (i.e. ACE2+). Titration experiments were replicated twice except for the "1 freeze/thaw cycle" for which titrations were replicated 4 times. Error bars represent 1 standard deviation of mean values.

Figure 4: Neutralization of SARS-CoV-2 and SARS-CoV pseudoviruses with soluble ACE2 and NAbs

a. Illustration of Spike protein pseudovirus blocked by soluble ACE2 or neutralizing antibodies. **B.** SARS-CoV-2 and SARS-CoV pseudovirus neutralization with soluble ACE2. SARS-CoV-2 RFP and SARS-CoV GFP pseudoviruses were pre-incubated with soluble ACE2 for 1 hour and added to 293 cells expressing ACE2-IRES-GFP or ACE2-mKO2 fusion, respectively. **c.** Neutralization of SARS-CoV-2 and SARS-CoV with S-RBD specific antibodies and soluble ACE2 (sACE2). Viruses were pre-incubated with antibodies (NAb#1 and SARS-CoV-2 S-RBD non-Nab) or soluble ACE2 (sACE2) proteins for 1 hour at the concentrations shown and subsequently added to target cells. Expression of RFP was determined at day 3 post-infection. Infection percentages were normalized to negative controls which are the infection conditions with no blocking agent. **d.** Neutralization of SARS-CoV-2 pseudoviruses using 4 different S-RBD NAbs and 2 different soluble ACE2 proteins. NAb #1 and #4 were human antibodies whereas NAb #2 and #3 were

557 mouse. Graphs in figures **c** and **d** represent 3 replicates of the experiments. Error bars indicate
558 one standard deviation of mean values.
559
560 **Figure 5: Neutralizing titers for SARS-CoV-2 and SARS-CoV in COVID-19 subject plasma**
561 **a.** Neutralization assay with S-RBD specific NAb, healthy control plasma, and a COVID-19 patient
562 plasma. 3-fold serial dilutions of NAb from 10 μg/ml to 1 ng/ml or the plasma from 1:10 to 1:10,000
563 were pre-incubated with Spike protein pseudovirus and added to 293-ACE2 cells. GFP
564 expression was analyzed by flow cytometry 3 days post infection. **b.** SARS-CoV-2 neutralization
565 titers (NT50) of COVID-19 plasma grouped as outpatient, hospitalized, ICU or deceased and
566 convalescent plasma donor groups. **c.** NT50 of COVID-19 patient and plasma donor groups
567 subdivided into males and females. **d.** Comparison of NT50 of COVID-19 plasma for SARS-CoV-
568 2 and SARS-CoV neutralization. SARS-CoV-2 or SARS-CoV pseudoviruses were pre-incubated
569 with COVID-19 plasma from all severity groups (n=104), 293-ACE2 cells were infected and RFP
570 expression was determined at day 3 using flow cytometry. **e.** Graph of SARS-CoV-2 NT50 values
571 from hospitalized subjects plotted against SARS-CoV. Two-tailed Mann-Whitney U test was used
572 to determine the statistical significances in figures **b**, **c** and **d** and two-tailed Spearman's was
573 used for figure **e**. Horizontal bars in **b, c** and **d** indicate mean values.
574
575 **Figure 6: Correlations of antibody, neutralization levels and COVID-19 subject**
576 **characteristics**
577 **a.** Neutralization (NT50) of COVID-19 plasma correlated with S-RBD IgG, S-RBD IgA, S-RBD
578 IgM and Nucleocapsid IgG. **b.** Correlation of NT50 with S-RBD specific IgG subclasses; IgG1,
579 IgG2, IgG3 and IgG4. **c.** Correlation of S-RBD IgG, Nucleocapsid IgG, S-RBD IgA and NT50 with
580 Age. Two-tailed Spearman's was used to determine statistical significances.
581

Supplementary Figure legends

Supplementary Figure 1: SARS-CoV-2 S-RBD antibody detection

a. Antibody assay measuring the plasma reactivity to S-RBD. Flow cytometry analysis of the PE fluorescence conjugated to anti-human IgG recognizing antibodies, present in the patient plasma and bound to S-RBD protein on the beads. Means of PE values in reciprocal dilutions were used to generate a curve for each positive plasma. Subject plasma with high and low antibody levels and a healthy control plasma were color-coded. **b.** Correlation of S1 subunit IgG, S1 N Terminal Domain (NTD) IgG, S2 Extracellular Domain (ECD) IgG and Nucleocapsid IgG with S-RBD IgG. **c**. Correlation of S-RBD IgA with S-RBD IgG. Two-tailed Spearman's was used to determine statistical significances. **d**. Heat map represents AUC values of Nucleocapsid (N) protein IgG, S-RBD IgG, S-RBD IgG subclasses and S-RBD IgA antibodies from individual subjects clustered as outpatients, hospitalized and ICU or deceased.

Supplementary Figure 2: ACE2 detection on cell surface membrane

a. Wild type or ACE2-IRES-GFP over-expressing 293 cells were stained with SARS-CoV-2 S1 protein fused to mouse Fc, and anti-mouse Fc secondary antibody. **B**. ACE2 expression, detected as in **a**, in wild type and ACE2 overexpressing 293 cells compared in an overlay of flow data.

Supplementary Figure 3: Neutralization of SARS-CoV-2 and SARS-CoV pseudoviruses

a. Normalized percent infection levels of SARS-CoV-2 and SARS-CoV pseudoviruses in neutralization assay using soluble ACE2 at 1 μg/mL, 3 μg/mL and 10 μg/mL concentrations. Significance was determined using two-tailed Mann-Whitney U test.

Supplementary Figure 4: S-RBD IgG subclasses correlation with total S-RBD IgG

a. Correlation of AUC levels of S-RBD specific IgG subclasses (IgG 1-4) with S-RBD specific total IgG. b. Correlation graphs of S-RBD IgG and NT50 with the number of days between PCR confirmation and the blood draw. Two-tailed Spearman's was used to determine the statistical significance.

Supplementary Figure 5: SARS-CoV-2 NT50 correlation with SARS-CoV NT50

a. Correlation of SARS-CoV-2 NT50 with SARS-CoV when all severity groups were combined, or only outpatient and plasma donor subjects were combined. **b**. SARS-CoV neutralization titers (NT50) of COVID-19 plasma grouped as outpatient, hospitalized, ICU or deceased and convalescent plasma donor groups. Two-tailed Spearman's was used for statistical analysis.

References

1 Hoffmann, M. *et al.* SARS-CoV-2 Cell Entry Depends on ACE2 and TMPRSS2 and Is Blocked by a Clinically Proven Protease Inhibitor. *Cell* **181**, 271-280 e278, doi:10.1016/j.cell.2020.02.052 (2020).

2 Robbiani, D. F. *et al.* Convergent antibody responses to SARS-CoV-2 in convalescent individuals. *Nature*, doi:10.1038/s41586-020-2456-9 (2020).

3 Rogers, T. F. *et al.* Isolation of potent SARS-CoV-2 neutralizing antibodies and protection from disease in a small animal model. *Science*, doi:10.1126/science.abc7520 (2020).

4 Wu, Y. *et al.* Identification of Human Single-Domain Antibodies against SARS-CoV-2. *Cell Host Microbe* **27**, 891-898 e895, doi:10.1016/j.chom.2020.04.023 (2020).

5 Wang, C. *et al.* A human monoclonal antibody blocking SARS-CoV-2 infection. *Nat Commun* **11**, 2251, doi:10.1038/s41467-020-16256-y (2020).

6 Seydoux, E. *et al.* Analysis of a SARS-CoV-2-Infected Individual Reveals Development of Potent Neutralizing Antibodies with Limited Somatic Mutation. *Immunity*, doi:10.1016/j.immuni.2020.06.001 (2020).

7 Cao, Y. *et al.* Potent neutralizing antibodies against SARS-CoV-2 identified by high-throughput single-cell sequencing of convalescent patients' B cells. *Cell*, doi:10.1016/j.cell.2020.05.025 (2020).

8 Hassan, A. O. *et al.* A SARS-CoV-2 Infection Model in Mice Demonstrates Protection by Neutralizing Antibodies. *Cell*, doi:10.1016/j.cell.2020.06.011 (2020).

9 Zost, S. J. *et al.* Potently neutralizing and protective human antibodies against SARS-CoV-2. *Nature* **584**, 443-449, doi:10.1038/s41586-020-2548-6 (2020).

10 Wu, Y. *et al.* A noncompeting pair of human neutralizing antibodies block COVID-19 virus binding to its receptor ACE2. *Science* **368**, 1274-1278, doi:10.1126/science.abc2241 (2020).

11 Liu, L. *et al.* Potent neutralizing antibodies against multiple epitopes on SARS-CoV-2 spike. *Nature* **584**, 450-456, doi:10.1038/s41586-020-2571-7 (2020).

12 Duan, K. *et al.* Effectiveness of convalescent plasma therapy in severe COVID-19 patients. *Proc Natl Acad Sci U S A* **117**, 9490-9496, doi:10.1073/pnas.2004168117 (2020).

13 Barone, P. & DeSimone, R. A. Convalescent plasma to treat coronavirus disease 2019 (COVID-19): considerations for clinical trial design. *Transfusion* **60**, 1123-1127, doi:10.1111/trf.15843 (2020).

14 Bloch, E. M. *et al.* Deployment of convalescent plasma for the prevention and treatment of COVID-19. *J Clin Invest* **130**, 2757-2765, doi:10.1172/JCI138745 (2020).

15 Chen, B. & Xia, R. Early experience with convalescent plasma as immunotherapy for COVID-19 in China: Knowns and unknowns. *Vox Sang*, doi:10.1111/vox.12968 (2020).

16 Lisboa Bastos, M. *et al.* Diagnostic accuracy of serological tests for covid-19: systematic review and meta-analysis. *Bmj*, doi:10.1136/bmj.m2516 (2020).

17 Huang, A. T. *et al.* A systematic review of antibody mediated immunity to coronaviruses: antibody kinetics, correlates of protection, and association of antibody responses with severity of disease. *medRxiv*, doi:10.1101/2020.04.14.20065771 (2020).

18 Hicks, J. *et al.* Serologic cross-reactivity of SARS-CoV-2 with endemic and seasonal Betacoronaviruses. *medRxiv*, doi:10.1101/2020.06.22.20137695 (2020).

19 Nagappa, B. & Marimuthu, Y. Seroconversion rate and diagnostic accuracy of serological tests for COVID-19. *Clin Infect Dis*, doi:10.1093/cid/ciaa676 (2020).

20 Che, X. Y. *et al.* Antigenic cross-reactivity between severe acute respiratory syndrome-associated coronavirus and human coronaviruses 229E and OC43. *J Infect Dis* **191**, 2033-2037, doi:10.1086/430355 (2005).

21 St John, A. L. & Rathore, A. P. S. Early Insights into Immune Responses during COVID-19. *J Immunol*, doi:10.4049/jimmunol.2000526 (2020).

22 Yazdanpanah, F., Hamblin, M. R. & Rezaei, N. The immune system and COVID-19: Friend or foe? *Life Sci* **256**, 117900, doi:10.1016/j.lfs.2020.117900 (2020).

23 Tong, P. B., Lin, L. Y. & Tran, T. H. Coronaviruses pandemics: Can neutralizing antibodies help? *Life Sci* **255**, 117836, doi:10.1016/j.lfs.2020.117836 (2020).

24 Deeks, J. J. *et al.* Antibody tests for identification of current and past infection with SARS-CoV-2. *Cochrane Database Syst Rev* **6**, CD013652, doi:10.1002/14651858.CD013652 (2020).

25 Siracusano, G., Pastori, C. & Lopalco, L. Humoral Immune Responses in COVID-19 Patients: A Window on the State of the Art. *Front Immunol* **11**, 1049, doi:10.3389/fimmu.2020.01049 (2020).

26 Ma, H. *et al.* Serum IgA, IgM, and IgG responses in COVID-19. *Cell Mol Immunol*, doi:10.1038/s41423-020-0474-z (2020).

27 Zhao, J. *et al.* Antibody responses to SARS-CoV-2 in patients of novel coronavirus disease 2019. *Clin Infect Dis*, doi:10.1093/cid/ciaa344 (2020).

28 Wang, Y. *et al.* Kinetics of viral load and antibody response in relation to COVID-19 severity. *J Clin Invest*, doi:10.1172/JCI138759 (2020).

29 Long, Q. X. *et al.* Clinical and immunological assessment of asymptomatic SARS-CoV-2 infections. *Nat Med*, doi:10.1038/s41591-020-0965-6 (2020).

30 Long, Q. X. *et al.* Antibody responses to SARS-CoV-2 in patients with COVID-19. *Nat Med* **26**, 845-848, doi:10.1038/s41591-020-0897-1 (2020).

31 Wang, Q. *et al.* Structural and Functional Basis of SARS-CoV-2 Entry by Using Human ACE2. *Cell* **181**, 894-904 e899, doi:10.1016/j.cell.2020.03.045 (2020).

32 Walls, A. C. *et al.* Structure, Function, and Antigenicity of the SARS-CoV-2 Spike Glycoprotein. *Cell* **181**, 281-292 e286, doi:10.1016/j.cell.2020.02.058 (2020).

33 Ou, X. *et al.* Characterization of spike glycoprotein of SARS-CoV-2 on virus entry and its immune cross-reactivity with SARS-CoV. *Nat Commun* **11**, 1620, doi:10.1038/s41467-020-15562-9 (2020).

34 Lv, H. *et al.* Cross-reactive antibody response between SARS-CoV-2 and SARS-CoV infections. *bioRxiv*, doi:10.1101/2020.03.15.993097 (2020).

35 Pinto, D. *et al.* Cross-neutralization of SARS-CoV-2 by a human monoclonal SARS-CoV antibody. *Nature*, doi:10.1038/s41586-020-2349-y (2020).

36 Zost, S. J. *et al.* Rapid isolation and profiling of a diverse panel of human monoclonal antibodies targeting the SARS-CoV-2 spike protein. *Nat Med* **26**, 1422-1427, doi:10.1038/s41591-020-0998-x (2020).

37 Wec, A. Z. *et al.* Broad neutralization of SARS-related viruses by human monoclonal antibodies. *Science* **369**, 731-736, doi:10.1126/science.abc7424 (2020).

38 Schmidt, F. *et al.* Measuring SARS-CoV-2 neutralizing antibody activity using pseudotyped and chimeric viruses. *J Exp Med* **217**, doi:10.1084/jem.20201181 (2020).

39 Crawford, K. H. D. *et al.* Protocol and Reagents for Pseudotyping Lentiviral Particles with SARS-CoV-2 Spike Protein for Neutralization Assays. *Viruses* **12**, doi:10.3390/v12050513 (2020).

40 Nie, J. *et al.* Establishment and validation of a pseudovirus neutralization assay for SARS-CoV-2. *Emerg Microbes Infect* **9**, 680-686, doi:10.1080/22221751.2020.1743767 (2020).

41 Padoan, A. *et al.* IgA-Ab response to spike glycoprotein of SARS-CoV-2 in patients with COVID-19: A longitudinal study. *Clin Chim Acta* **507**, 164-166, doi:10.1016/j.cca.2020.04.026 (2020).

42 Ejemel, M. *et al.* IgA MAb blocks SARS-CoV-2 Spike-ACE2 interaction providing mucosal immunity. *bioRxiv*, doi:10.1101/2020.05.15.096719 (2020).

43 Woodruff, M. C. *et al.* Extrafollicular B cell responses correlate with neutralizing antibodies and morbidity in COVID-19. *Nat Immunol*, doi:10.1038/s41590-020-00814-z (2020).

44 Ulrich, H., Pillat, M. M. & Tarnok, A. Dengue Fever, COVID-19 (SARS-CoV-2), and Antibody-Dependent Enhancement (ADE): A Perspective. *Cytometry A*, doi:10.1002/cyto.a.24047 (2020).

45 Roschewski, M. *et al.* Inhibition of Bruton tyrosine kinase in patients with severe COVID-19. *Sci Immunol* **5**, doi:10.1126/sciimmunol.abd0110 (2020).

46 Chen, X. *et al.* Functional Interrogation of Primary Human T Cells via CRISPR Genetic Editing. *J Immunol* **201**, 1586-1598, doi:10.4049/jimmunol.1701616 (2018).

47 Karasawa, S., Araki, T., Nagai, T., Mizuno, H. & Miyawaki, A. Cyan-emitting and orange-emitting fluorescent proteins as a donor/acceptor pair for fluorescence resonance energy transfer. *Biochem J* **381**, 307-312, doi:10.1042/BJ20040321 (2004).

48 Sakaue-Sawano, A. *et al.* Visualizing spatiotemporal dynamics of multicellular cell-cycle progression. *Cell* **132**, 487-498, doi:10.1016/j.cell.2007.12.033 (2008).

49 Ratner, B. The correlation coefficient: Its values range between +1/−1, or do they? *Journal of Targeting, Measurement and Analysis for Marketing* **17**, 139-142, doi:10.1057/jt.2009.5 (2009).

Figure 1

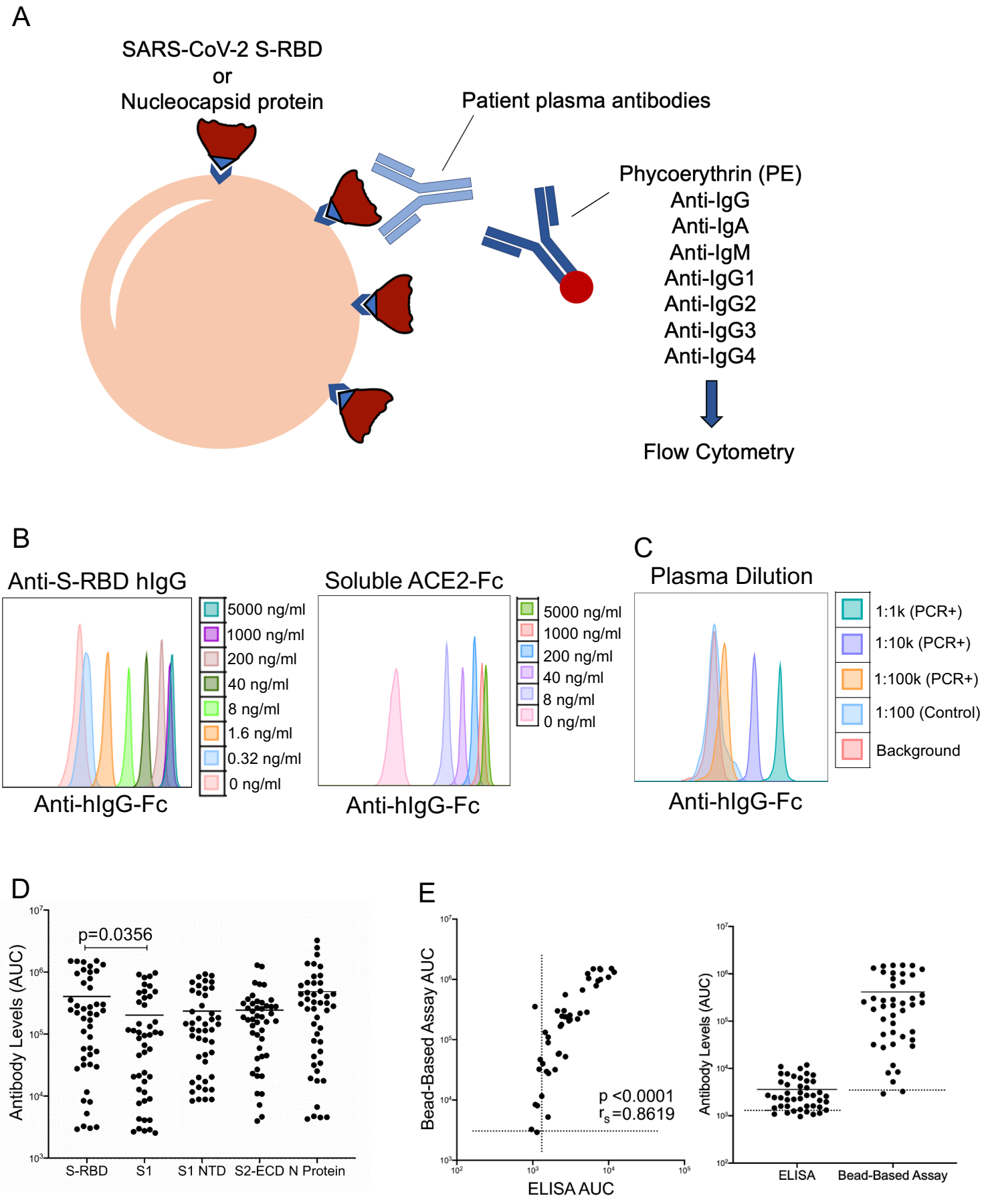

Figure 2

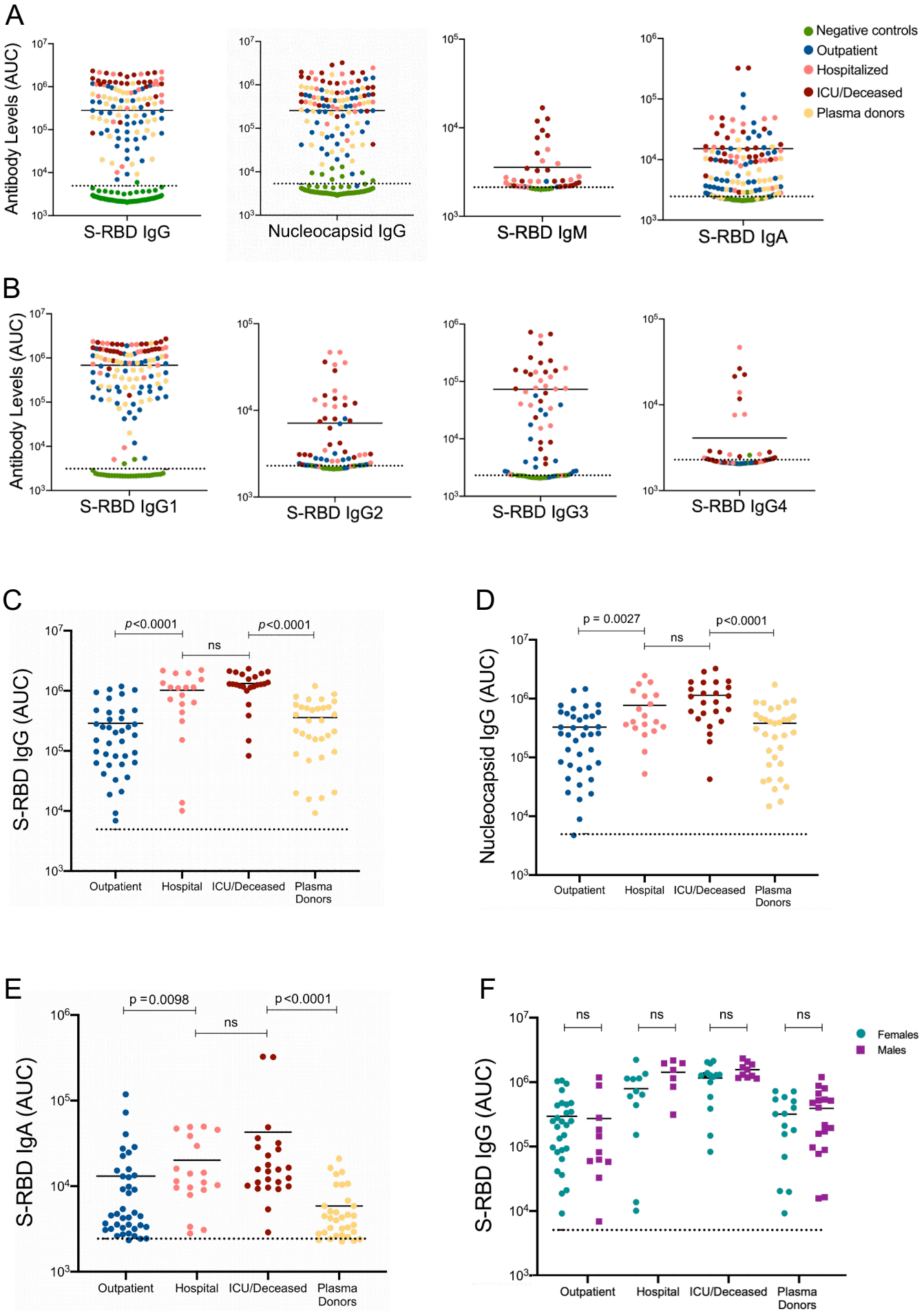

Figure 3

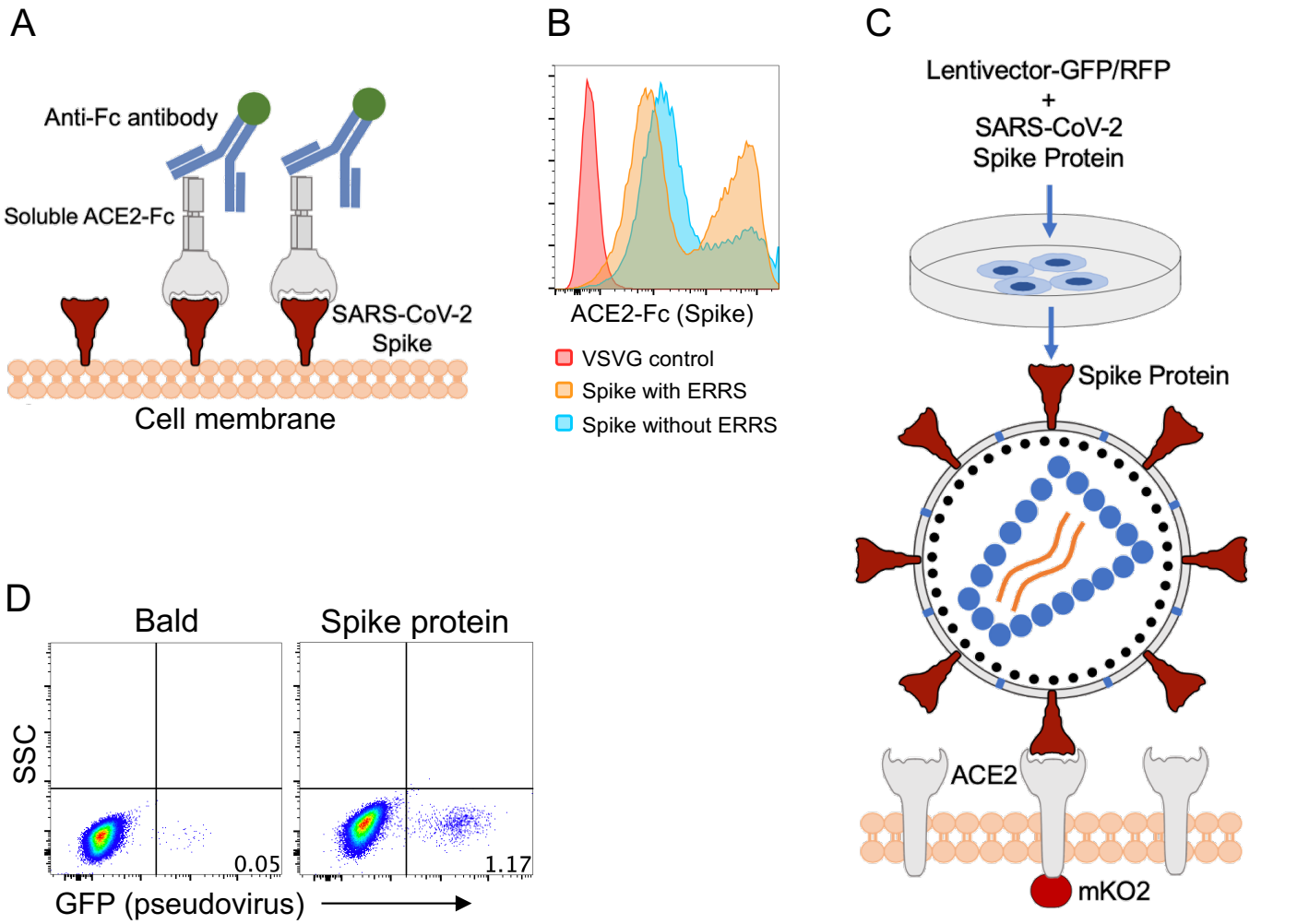

Figure 4

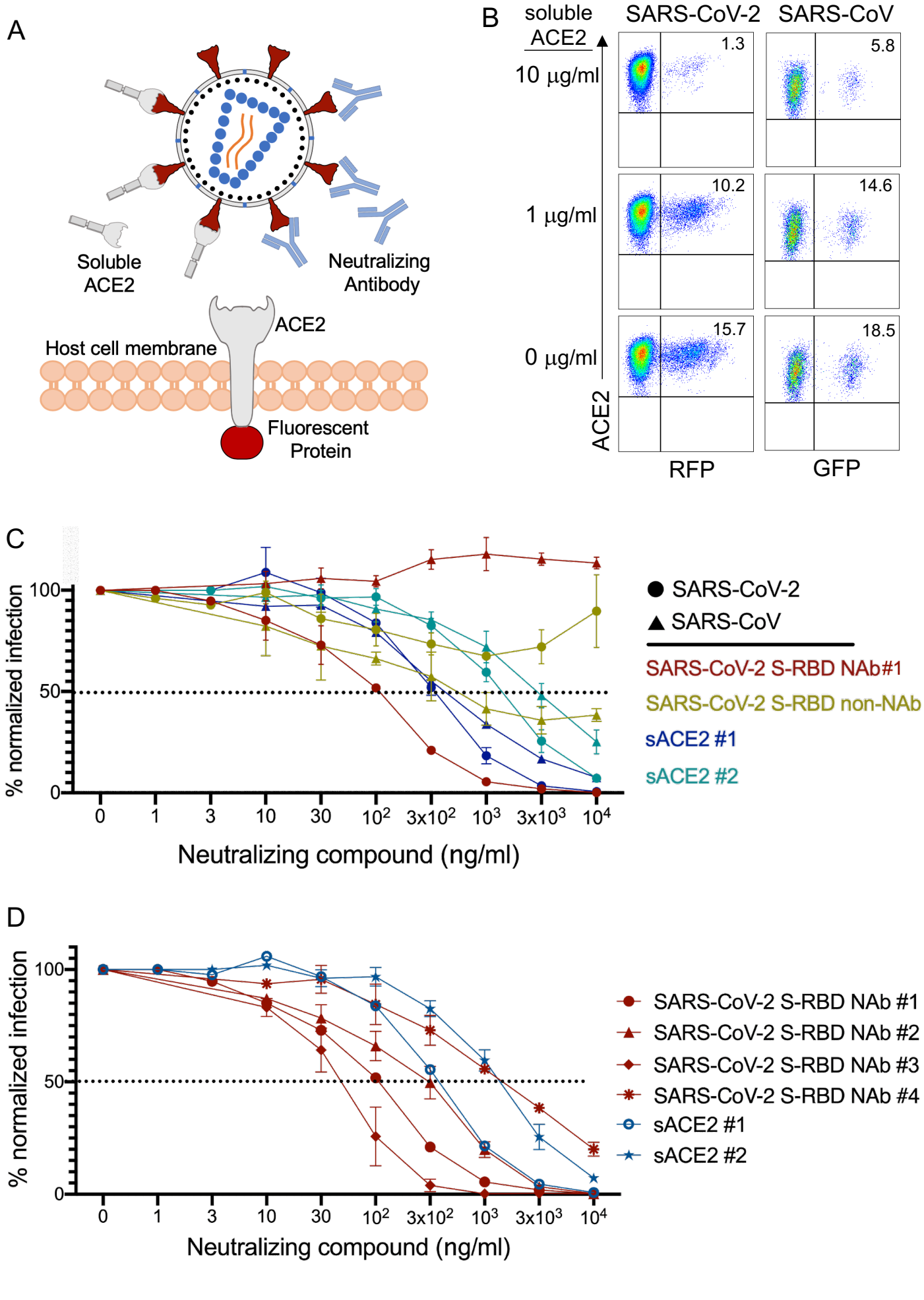

Figure 5

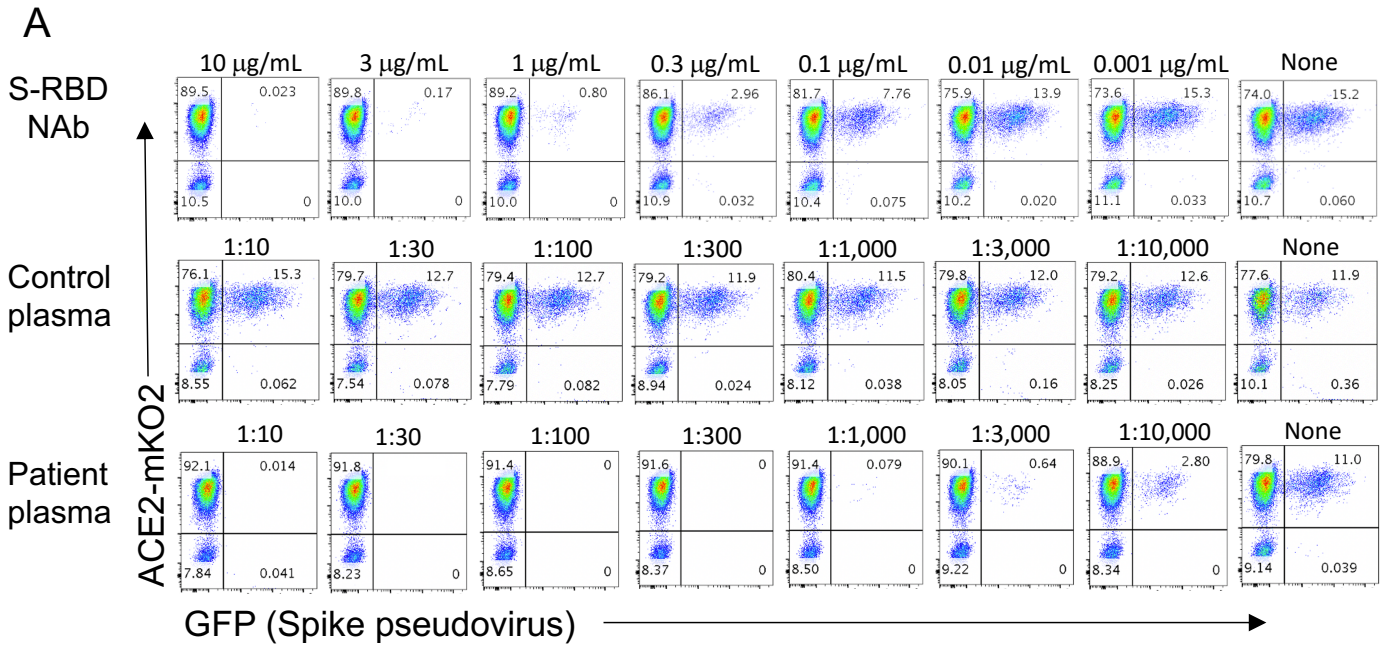

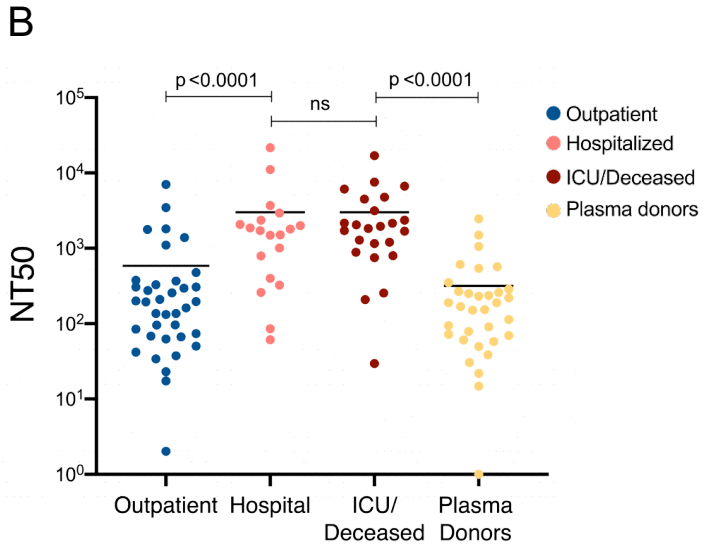

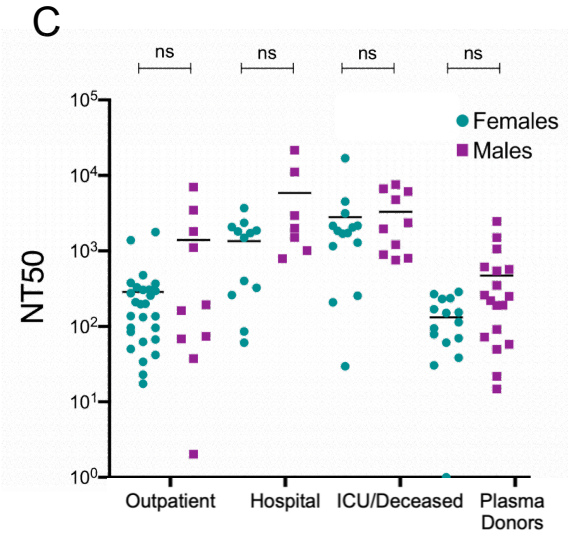

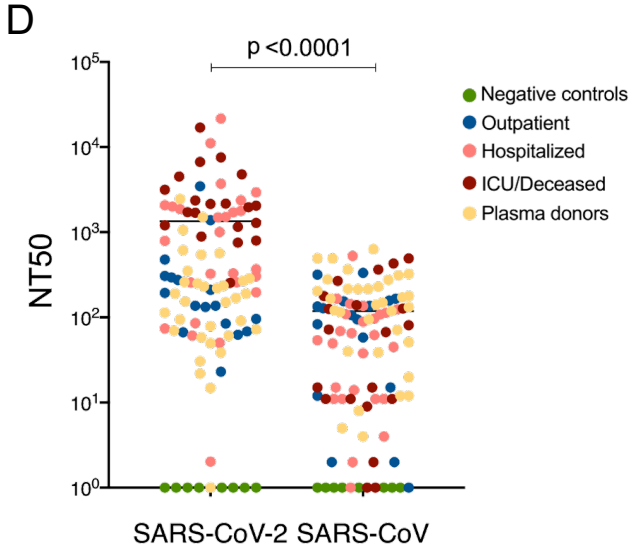

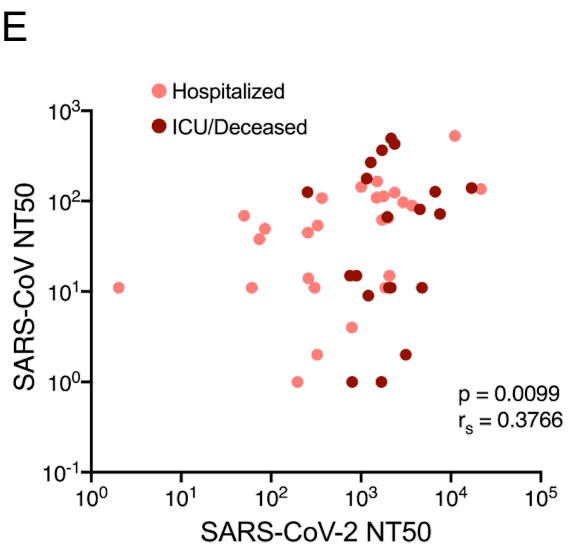

Figure 6

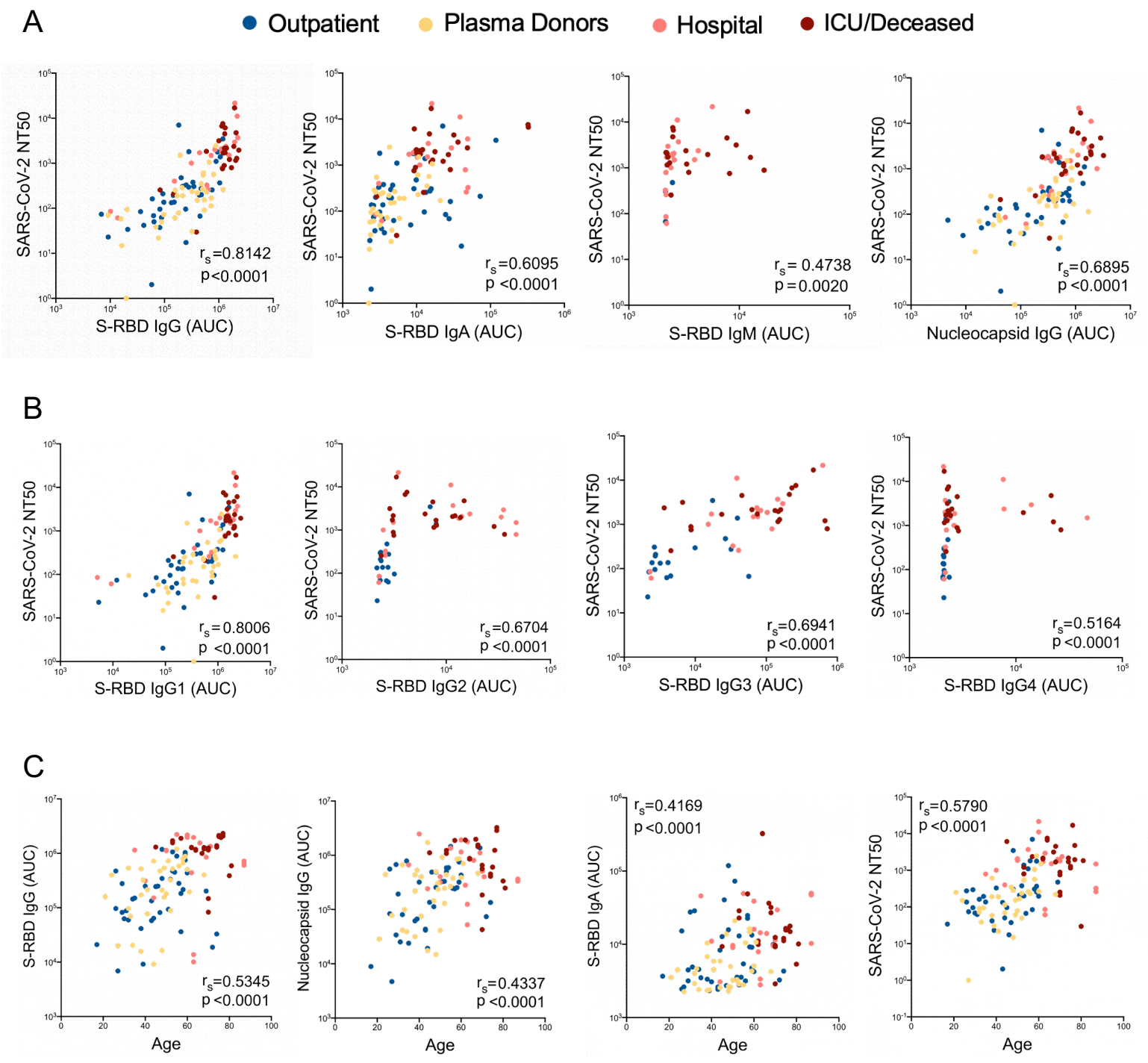

Supplementary Figure 1

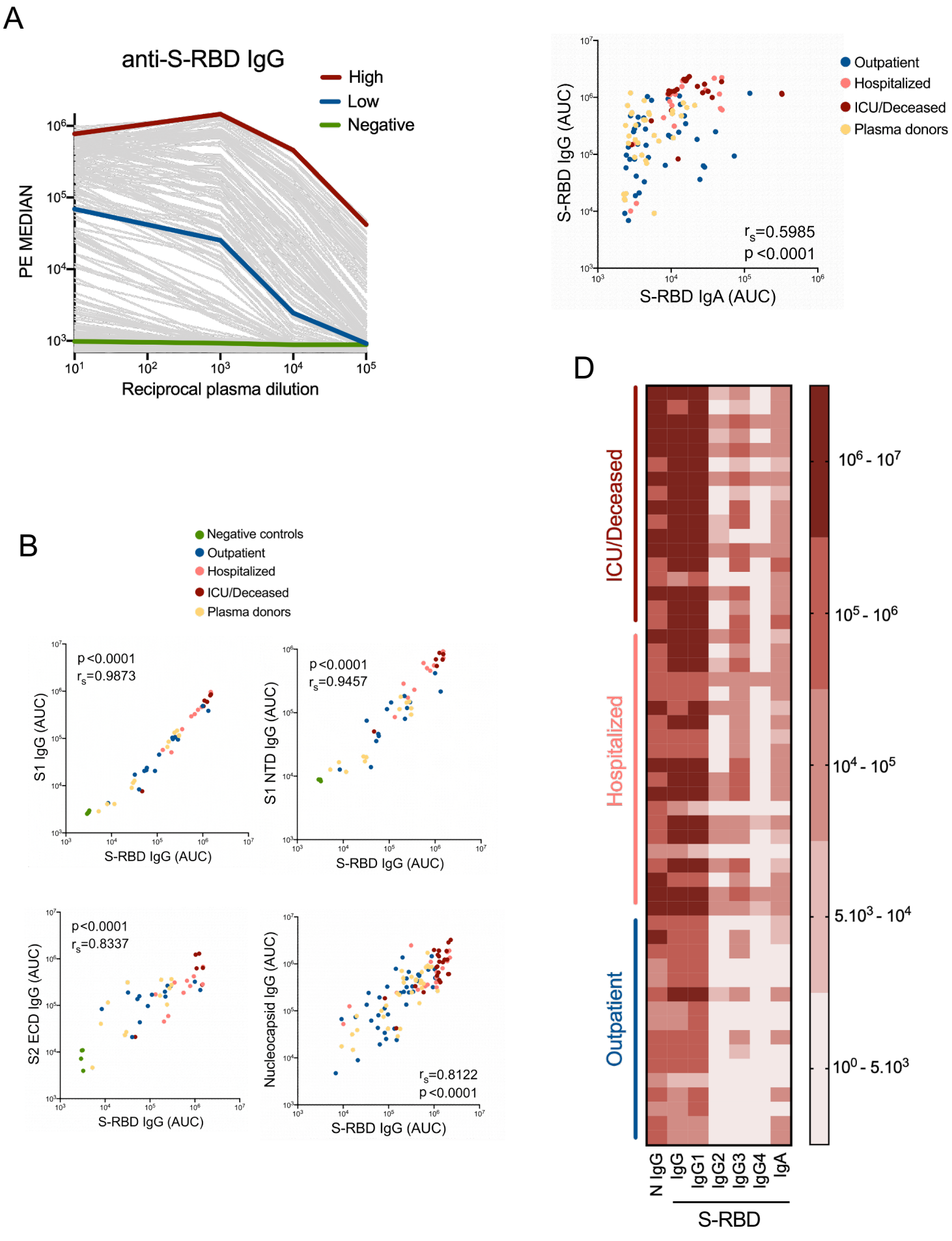

Supplementary Figure 2

A

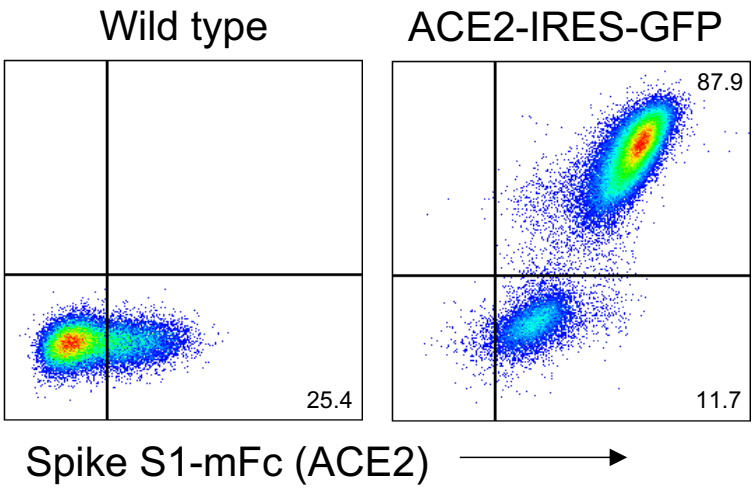

B

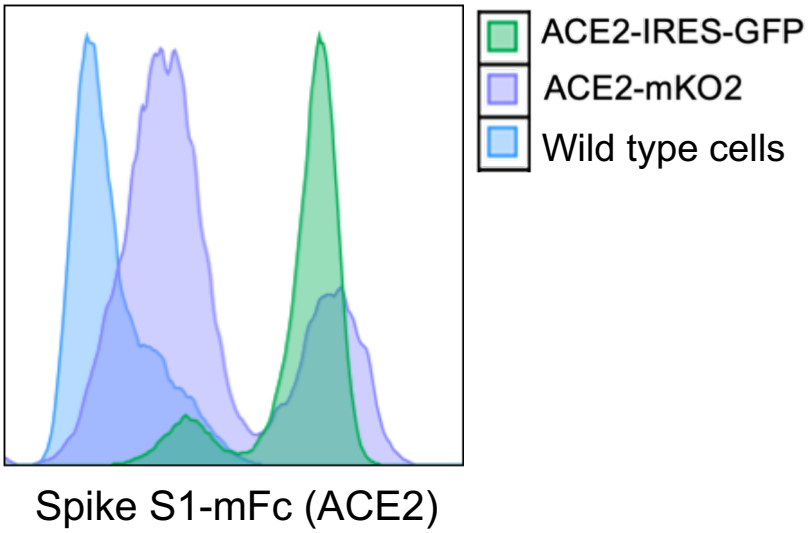

Supplementary Figure 3

A

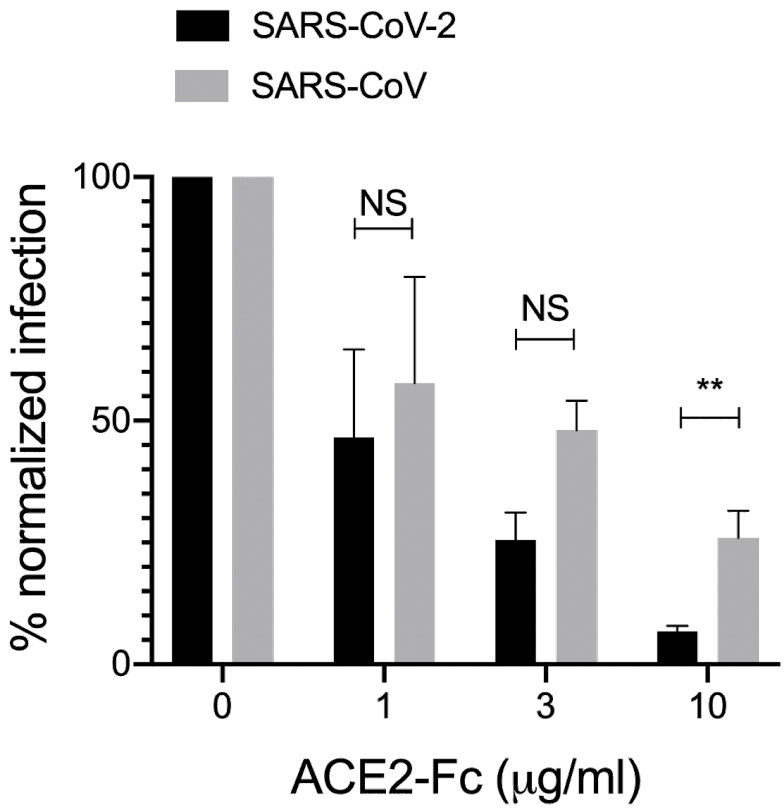

Supplementary Figure 4

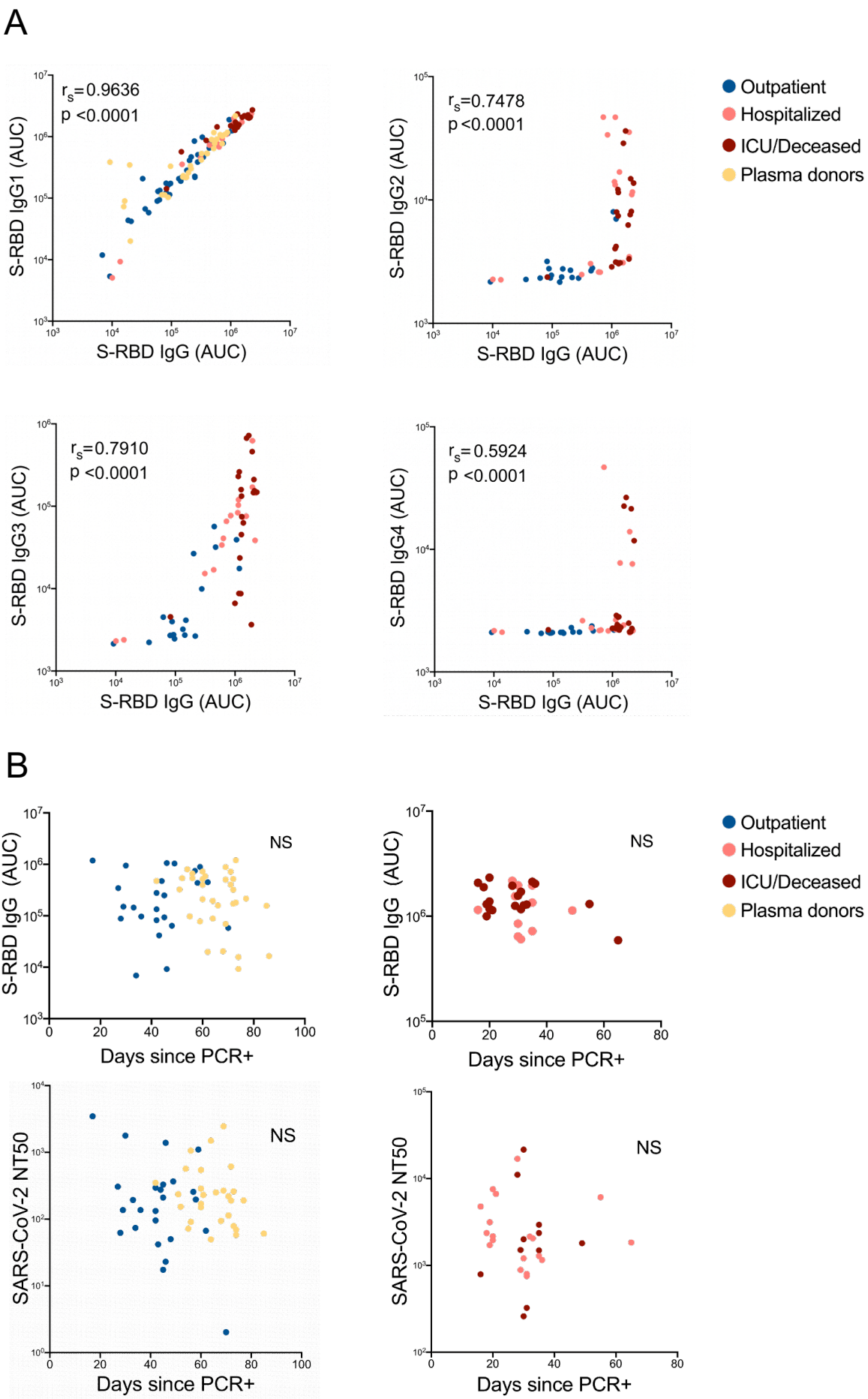

Supplementary Figure 5